24th COBEM - 2017

24th ABCM International Congress of Mechanical Engineering
December 3-8, 2017, Curitiba, PR, Brazil

COBEM-2017-2053
THE INFLUENCE OF A CRACK ON THE DYNAMIC BEHAVIOR OF A FLEXIBLE DISC

Bruno Resende Ferreira Rende
Izabela Batista da Silva
Tobias Souza Morais
Aldemir Ap Cavalini Jr
Valder Steffen Jr
LMEst - Structural Mechanics Laboratory, Federal University of Uberlândia, School of Mechanical Engineering, Av. João Naves de Ávila, 2121, Uberlândia, MG, 38408-196, Brazil.
e-mail: brunorende@ufu.br, izabela.silva@ufu.br, tobias@ufu.br, aacjunior@ufu.br, vsteffen@ufu.br

Abstract. *The present work aims at evaluating the effects of crack on the dynamic behavior of a flexible rotating beam. The development, solution, and analysis of a system composed by a flexible rotor (mass-spring system) attached to four flexible blades is presented. The flexible blades are modeled as Euler-Bernoulli beams with tip masses at their ends. In this case, a linear beam model is associated with second order non-linear terms. The equations of motion of the entire rotor-blade system were obtained by applying the Newton-Euler-Jourdain method. The crack presence in the blade brings an additional flexibility, which is introduced in the blade model by using a torsional spring. The resulting blade stiffness is obtained through the equation of the beam elastic curve. The Newmark time integration method associated with the Newton-Raphson iteration procedure are used to solve the equations of motion. Two different scenarios were evaluated, considering both the healthy and cracked blade conditions. Finally, the dynamic responses of the rotor-blade system are shown in time and frequency domains, as well as the instability map.*

Keywords: *rotor and flexible blades, transversal crack, frequency and time domain analyzes, instability.*

1. INTRODUCTION

Flexible blades coupled to rotating shafts are widely used in industrial machines, such as compressors, exhausters, and turbines. These components are usually exposed to different operating conditions, including high-speed situations, large centrifugal forces, high temperatures, and high pressures (Xu et al., 2016). Thus, associated with the inevitable manufacturing flaws, a crack can emerge and grow mainly at the blades. Consequently, the chances of the entire system to collapse increase. In those cases, the application of predictive maintenance becomes necessary. Nowadays, there are various methods used for crack detection, such as the ultrasonic, X-rays, and acoustic emission (Wu and Huang, 1998). These methods have not proved to be efficient in some situations due to the required detailed periodic inspection, which is very costly according to Saavedra and Cuitiño (2001). Thus, this problem led to investigations on a class of crack detection methods based on vibration analysis through either frequency or time domain responses.

The present work aims to investigate the influence of cracks on the dynamic behavior of a rotor-blade system. There are contributions in the literature on the modeling of flexible blades. Legrand (2005) formulated a finite element model considering the blades attached to the rotor by torsional springs. The blades were linked with each other by a linear spring. Santos et al. (2004) and Saracho (2002) used an alternative approach based on the Newton-Euler-Jourdain's equation to obtain the equations of motion of a rotor-blade system. The authors pointed out that, as the blades are flexible, their deformation cannot be neglected because the coupling between the displacement of the blades and their deformation causes an effect known as centrifugal stiffening. This effect makes the natural frequencies of the rotating beam to increase according to the rotating speed, which is the main characteristic observed in the dynamic behavior of this kind of system.

The dynamic behavior of cantilever beams with transversal cracks was extensively discussed in various papers. Wu and Huang (1998) employed an energy approach followed by the Extended Hamilton's principle in conjunction with a weighted residual method to obtain the equations of motion of a cracked beam. Dimarogonas (1976) and Chondros (1977) explained that the crack generates a new local flexibility in the beam. The authors used the linear fracture mechanics theory to represent the crack. Dimarogonas et al. (1990) also observed that the principal effect introduced by

cracks on beams is a new local flexibility that changes the dynamical behavior of the system. Dimarogonas et al. (1990) formulated a model constituted by two beams connected by a torsional spring to represent this effect, whose stiffness coefficient represents the crack. Dimarogonas et al. (1990) and Dimarogonas and Paipetis (1983) used the crack strain energy function to determine the additional local flexibility on the beam. Mayes and Davies (1984) analyzed the influence of cracks in a rotor shaft. The authors used a finite element model to include the new local flexibility in the shaft, in which the diameter of the shaft finite element was reduced at the crack position according to the crack flexibility.

In the present paper, the adopted model of the rotor-blade system is similar to the one described by Saracho (2002). The model is composed by a mass-spring system that represents the rotor and by four rotating beams with tip masses attached to them. The blades are modeled as Euler-Bernoulli beams (Santos et al., 2004) and their deformations are obtained considering second order non-linear terms to ensure that the centrifugal stiffness is correctly represented (Simo and Vu Quoc, 1986). A second order-linearized model is then obtained. The Newton-Euler-Jourdain method was applied to determine the equations of motion of the rotor-blade system. The crack is represented by an additional local flexibility of the blade according to the formulation presented by Dimarogonas et al. (1990). The equations of motion are solved by using the Newmark time integration method and Newton-Raphson iteration technique for two different scenarios. The first one evaluates the rotor-blade system without crack (pristine condition) and the second scenario considers a crack in one of the blades. The vibration responses both in time and frequency domains are obtained, so that a comparison between the scenarios is performed.

2. ROTOR-BLADE MODEL

The model used to represent the coupling between the rotor and the four flexible blades is shown in Fig. 1. As can be seen, the model is composed by a rotor with mass m_0 and radius r, which is elastically supported by the stiffness k_0, and four blades with lengths L_i (the blades present thickness h_i) and stiffness k_i (i = 1, 2, 3, 4). Tip masses m_{pi} are attached to the blades, presenting length L_{ti} and width b_{ti}; r_{ti} represents the distance between the extremity and the centroid of the tip mass. The system has five degrees of freedom $Z(t) = \{z_0(t)\ z_1(t)\ z_2(t)\ z_3(t)\ z_4(t)\}^T$, where $z_0(t)$ represents the horizontal displacement of the rotor (point C in Fig. 1a) and $z_i(t)$ describes the displacements of the blades.

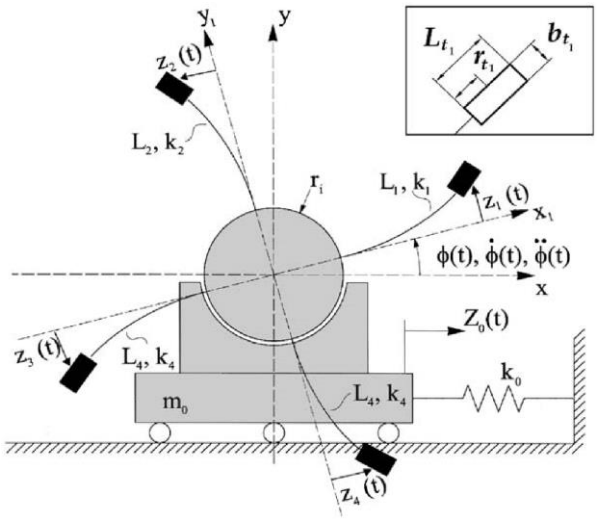

Fig 1. Model illustrating the rotor-blade system (Santos et al., 2004).

Three reference frames are used to obtain the equations of motion of the rotor-blade system (Saracho, 2002), namely, the inertial frame B_I (x, y, z), the rotating frame B_1 (x_1, y_1, z_1) centered at the point C (defining the angular position ϕ through the x_1 axis), and the frame B_{pi} (x_{pi}, y_{pi}, z_{pi}) that is fixed to each tip mass.

According to Santos et al. (2004), the B_{pi} frame facilitates the description of the beam deformation field. Therefore, this frame was employed to find the displacements and the external forces of each blade p_i. The displacements of the blades are interpolated by using a cubic polynomial form to minimize the number of degrees of freedom of the model and to approximate only the first bending mode of the blade. The displacements are given by Eq. (1).

$$ {}_{B_{pi}}\mathbf{u}_{p_i} = \begin{pmatrix} 0 \\ 0 \\ \psi_i(\xi_i) z_i(t) \end{pmatrix} \qquad \psi_i(\xi_i) = \frac{3}{2}\left(\frac{\xi_i}{L_i}\right)^2 - \frac{1}{2}\left(\frac{\xi_i}{L_i}\right)^3 \tag{1} $$

Then, the absolute velocity and the acceleration of each blade are given by Eq. (2) and Eq. (3), respectively.

$$ {}_{B_{pi}}\boldsymbol{v}_{p_i} = {}_{B_{pi}}\boldsymbol{v}_{O_i} + \frac{d}{dt}\left({}_{B_{pi}}\boldsymbol{u}_i\right) + {}_{B_{pi}}\boldsymbol{\omega} \times \left({}_{B_{pi}}\boldsymbol{L}_i + {}_{B_{pi}}\boldsymbol{u}_i\right) \tag{2} $$

$$ \begin{aligned} {}_{B_{pi}}\boldsymbol{a}_{p_i} = {}_{B_{pi}}\boldsymbol{a}_{O_i} + \frac{d^2}{dt^2}\left({}_{B_{pi}}\boldsymbol{u}_i\right) + 2\,{}_{B_{pi}}\boldsymbol{\omega} \times \left({}_{B_{pi}}\boldsymbol{u}_i\right) + {}_{B_{pi}}\dot{\boldsymbol{\omega}} \times \left({}_{B_{pi}}\boldsymbol{L}_i + {}_{B_{pi}}\boldsymbol{u}_i\right) \\ + {}_{B_{pi}}\boldsymbol{\omega} \times {}_{B_{pi}}\boldsymbol{\omega} \times \left({}_{B_{pi}}\boldsymbol{L}_i + {}_{B_{pi}}\boldsymbol{u}_i\right) \end{aligned} \tag{3} $$

where ${}_{B_{pi}}\boldsymbol{v}_{p_i}$, ${}_{B_{pi}}\boldsymbol{a}_{p_i}$ ${}_{B_{pi}}\boldsymbol{\omega}$, and ${}_{B_{pi}}\dot{\boldsymbol{\omega}}$, are the velocity and acceleration of the point where the blade is fixed to the rotor (point O_i), respectively, ${}_{B_{pi}}\boldsymbol{\omega}$ and ${}_{B_{pi}}\dot{\boldsymbol{\omega}}$ represents the angular speed and the angular acceleration of the rotor, respectively. These vectors are showed in Eq. (4). It is important to note that the only external force applied to the system is its own weight.

$$ {}_{B_{pi}}\boldsymbol{\omega} = \begin{Bmatrix} \dot{\varphi} \\ 0 \\ 0 \end{Bmatrix} \qquad {}_{B_{pi}}\dot{\boldsymbol{\omega}} = \begin{Bmatrix} \ddot{\varphi} \\ 0 \\ 0 \end{Bmatrix} \qquad {}_{B_{pi}}\boldsymbol{L}_i = \begin{Bmatrix} 0 \\ L_i \\ 0 \end{Bmatrix} \tag{4} $$

In the rotor-blade model, the rotatory inertia was considered. Thus, an equivalent mass is estimated as follows:

$$ \overline{m}_i = m_i\,\psi(L_i)^2 + \left(It_i + m_i\,rt_i\right)\psi'(L_i)^2 + 2m_i\,rt_i\,\psi(L_i)\psi'(L_i) \quad where\ It_i = m_i\left(\frac{Lt_i^2 + ht_i^2}{12}\right) \tag{5} $$

where $\psi(L_i)$ is the same cubical polynomial showed in Eq. (1).

The energy stored in the system was separated in two terms, π_0 that represents the energy of the elastic support and π_{pi}, which is the potential energy in the blades. In this case, $\pi_{pi} = \pi_{li} + \pi_{gi}$, where π_{li} is associated with the deformation of the blades and π_{gi} is the energy related to the blade geometrical stiffness. It is considered that π_{pi} ensures that the second non-linear terms of deformation vector are not neglected. The mentioned energy terms are given by:

$$ \pi_0 = \frac{1}{2}k_0\,z_0^2 \tag{6} $$

$$ \pi_{l_i} = \frac{1}{2}\int_0^{Li} EI\left(\frac{\partial^2}{\partial\xi_i^2}\left(\psi_i(\xi_i)z_i\right)\right)^2 d\,\xi_i = \frac{1}{2}k_i\,z_i^2\,, k_i = \frac{3EI}{L_i} \tag{7} $$

$$ \pi_{gi} = \frac{1}{2}\int_0^{Li} N_{pi}(\xi_i)\left(\frac{\partial^2}{\partial\xi_i^2}\left(\psi_i(\xi_i)z_i\right)\right)^2 d\xi_i = \frac{3}{5L_i}N_{pi}(\xi_i)\,z_i^2 \tag{8} $$

$$ \pi_{pi} = \pi_{li} + \pi_{gi} \tag{9} $$

where N_{pi} is the normal force acting on each blade. The expression of the normal force can be approximate to (Kane et al., 1987) by using the Eq. (10).

$$ N_{p_i}(\xi_i) = m_{p_i}\dot{\phi}^2(L_i + r) \tag{10} $$

Finally, to obtain the equations of motion, the Newton-Euler-Jourdain method is used. An eccentricity ε with an angular position φ is considered in the model. Then the equations of motion are written as:

$$ \mathbf{M}\ddot{\mathbf{q}} + (\mathbf{C} + \mathbf{C}_1)\dot{\mathbf{q}} + (\mathbf{K} + \mathbf{K}_\Omega + \mathbf{K}_\alpha + \mathbf{K}_g)\mathbf{q} = \mathbf{f}_\Omega + \mathbf{f}_\alpha + \mathbf{f}_p \tag{11} $$

in which $\mathbf{M}$ is the mass matrix, $\mathbf{C}_1$ is the coriolis matrix, $\mathbf{K}$ is the structural stiffness matrix, $\mathbf{K}_\Omega$ is the stiffness matrix due to the angular speed, $\mathbf{K}_\alpha$ is the stiffness due to angular acceleration, $\mathbf{K}_g$ is the geometric stiffness, $\mathbf{f}_\Omega$ is the force

vector associated to angular speed, $\mathbf{f}_\alpha$ is the force vector due to angular acceleration, and $\mathbf{f}_p$ is the weight force vector. Also, a proportional damping matrix **C** was added to the system, as shows by Eq. (12).

$$\mathbf{C} = \alpha\mathbf{M} + \beta\mathbf{K} \qquad \alpha = 5 \qquad \beta = 1x10^{-5} \tag{12}$$

3. CRACK MODEL

The structural stiffness **K** presented in Eq. (11) must be modified due to the local flexibility introduced by the crack. As performed by Dimarogonas et al. (1990), the blade was separated in two other beams (see Fig. 2b) which lengths are, $L_{B1} = L_1$ and $L_{B2} = L - L_{B1}$. These two new beams are also modeled as Euler-Bernoulli beams and linked by a torsional spring with stiffness coefficient k_T.

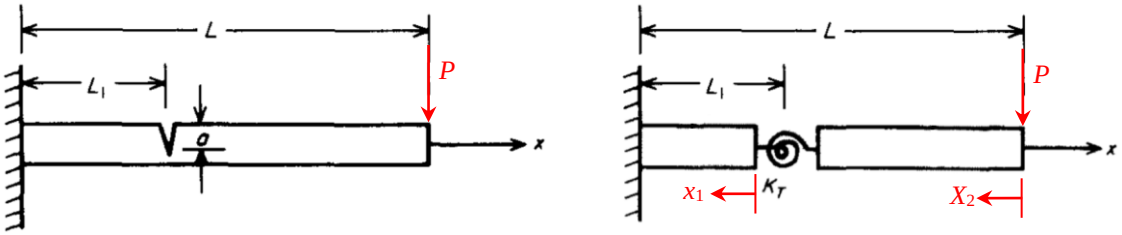

a) Crack depth and beam height. b) Model used to determine the stiffness.

Figure 2: Model used to represent the crack (Dimarogonas et al., 1990).

In order to determine the stiffness coefficient k_T according to the crack depth a and position along the blade (i.e., according to the length L_{B1}), it was considered that the beams had only bending movement, as shows the Eq. (13) and Eq. (14).

$$k_T = \frac{1}{c} \qquad c = \left(\frac{5.346h}{EI}\right) I\left(a/h\right) \tag{13}$$

$$\begin{aligned} I\left(a/h\right) = {} & 1.8624\,(a/h)^2 - 3.95\left(a/h\right)^3 + 16.375\left(a/h\right)^4 - 37.226\left(a/h\right)^5 + 76.81\left(a/h\right)^6 - 126.9\left(a/h\right)^7 \\ & + 172\left(a/h\right)^8 - 143.97\left(a/h\right)^9 + 66.56\left(a/h\right)^{10} \end{aligned} \tag{14}$$

where c is the compliance, h is the height of the beam, E and I are, respectively, the modulus of elasticity of the material and the moment of inertia of blade cross section. $I(a/h)$ is the dimensionless local compliance.

As can be seen in Fig. 2, the blade was divided in two beams, which lengths L_{B1} and L_{B2}, connected by the angular stiffness k_T to represent the cracked blade. Thus, an equivalent stiffness coefficient was determined considering the scheme presented in Fig. 2b, as shows Eq. (15).

$$k_{eq} = \frac{1}{\frac{1}{k_{B1}} + \frac{1}{k_{B2}} + \frac{1}{k_T}} \tag{15}$$

where k_{B1} is the stiffness of beam with length L_{B1} (beam #1) and k_{B2} is the stiffness of the beam with length L_{B2} (beam #2). It is worth mentioning that the coefficients k_{B1} and k_{B2} were obtained by using the Euler-Bernoulli theory for beams through the elastic line equation, given by:

$$\frac{d^2 y_1}{dx_1^2} = \frac{M}{EI} \qquad M = Px_1 + PL_{B2} \tag{16}$$

where y is the deflection of the beam, M is the bending moment applied to the beam, and P is a force applied in the end of the beam (see Fig. 2).

Integrating the Eq. (16) twice with respect to x_1 ($0 \leq x_1 \leq L_1$), the deflection α_1 of the beam #1 and the vertical displacement y_1 of the beam #1 are found:

$$\frac{dy_1}{dx_1} = \alpha_1 = \frac{Px_1{}^2}{2EI} + \frac{PL_{B2}x_1}{EI} + C_1 \qquad y_1(x_1) = \frac{Px_1{}^3}{6EI} + \frac{PL_{B2}x_1{}^2}{2EI} + C_1x_1 + C_2 \tag{17}$$

In Eq. (16), C_1 and C_2 are constants that can be evaluated considering that at $x_1 = L_{B1}$, the deflection and the displacement of the beam are zero, i.e., $\alpha_1 = 0$ and $y_1 = 0$. Thus,

$$C_1 = -\frac{P}{EI}\left(\frac{L_{B1}{}^2}{2} + L_{B1}L_{B2}\right) \qquad C_2 = \frac{P}{EI}\left(\frac{L_{B2}L_{B1}{}^2}{2} + \frac{L_{B1}{}^3}{3}\right) \tag{18}$$

Then,

$$y_1(x_1) = \frac{Px_1{}^3}{6EI} + \frac{PL_{B2}x_1{}^2}{2EI} - \frac{P}{EI}\left(\frac{L_{B1}{}^2}{2} + L_{B1}L_{B2}\right)x_1 + \frac{P}{EI}\left(\frac{L_{B2}L_{B1}{}^2}{2} + \frac{L_{B1}{}^3}{3}\right) \tag{19}$$

In Eq. (19), $k_{B1} = P/y_1(x_1)$ for $x_1 = 0$, as shows the Eq. (20).

$$k_{B1} = \frac{EI}{\left(\frac{L_{B2}L_{B1}{}^2}{2} + \frac{L_{B1}{}^3}{3}\right)} \tag{20}$$

The stiffness k_{B2} of the beam #2 can be found by using a similar procedure through Eq. (16). Then, for the beam #2 (Fig. 2b), with $0 \le x_2 \le L_2$, one has:

$$\frac{d^2y_2}{dx_2{}^2} = \frac{M}{EI} \qquad M = Px_2 \tag{21}$$

Integrating twice the Eq. (20) with respect to x_2, the deflection α_2 and the displacement y_2 are obtained as follows:

$$\frac{dy_2}{dx_2} = \alpha_2 = \frac{Px_2}{2EI} + C_3 \qquad y_2(x_2) = \frac{Px_2}{2EI} + C_3x_2 + C_4 \tag{22}$$

The constants C_3 and C_4 in Eq. (22) can be determined by using the boundary conditions associated with the beam #2. In this case, at $x_2 = L_{B2}$, the displacement of the beam #2 is equal to the displacement of beam #1, i.e., $y_2(L_{B2}) = y_1(0)$, and the deflection at the same point is the sum of the deflections of the beam #1 at $y_1(0)$ with the deflection due to the torsional spring:

$$\alpha_2(L_{B2}) = \alpha_1(0) + \phi \qquad \phi = \frac{PL_{B2}}{k_T} \tag{23}$$

$$C_3 = \frac{PL_{B2}}{k_T} - \frac{P}{EI}\left(\frac{L_{B2}{}^2}{2} + \frac{L_{B1}{}^2}{2} + L_{B1}L_{B2}\right) \qquad C_4 = \frac{P}{EI}\left(L_{B1}{}^2L_{B2} + \frac{L_{B1}{}^3}{3} + \frac{L_{B2}{}^3}{3} + L_{B1}L_{B2}{}^2\right) - \frac{PL_{B2}{}^2}{k_T} \tag{24}$$

Substituting these values in Eq. (22),

$$y_2(x_2) = \frac{Px_2{}^2}{6EI} + \frac{PL_{B2}}{k_T} - \left[\frac{P}{EI}\left(\frac{L_{B2}{}^2}{2} + \frac{L_{B1}{}^2}{2} + L_{B1}L_{B2}\right)\right]x_2 + \frac{P}{EI}\left(L_{B1}{}^2L_{B2} + \frac{L_{B1}{}^3}{3} + \frac{L_{B2}{}^3}{3} + L_{B1}L_{B2}{}^2\right) - \frac{PL_{B2}}{k_T} \tag{25}$$

The stiffness of the beam #2, k_{B2}, can be determined from P/y_2 in $x_2 = 0$ of Eq. (25). Thus,

$$k_{B2} = \frac{1}{\frac{1}{EI}\left({L_{B1}}^2 L_{B2} + \frac{{L_{B1}}^3}{3} + \frac{{L_{B2}}^3}{3} + L_{B1}{L_{B2}}^2 \right) - \frac{L_{B2}}{k_T}} \tag{26}$$

Finally, substituting Eq. (26), Eq. (20), and Eq. (13) in Eq. (15), the equivalent stiffness of the blade with a crack can be found.

4. NUMERICAL APPLICATION

Table 1 presents the parameters used to formulate the rotor-blade system that is studied in the present work. Aiming to verify the influence that the crack brings to the system, Eq. (11) was solved considering the healthy blade and the blade #1 with a crack with $L_{B1} = 0.05\ L_1$.

Table 1. Main parameters of the rotor-blade system.

Rotor			*Blades* (i = 1, 2, 3, 4)		
m_r	1.907	kg	θ_i	$(i-1)\pi/2$	rad
k_y	$2.16x10^4$	N/m	m_{pi}	0.1*	kg
r	0.04	m	k_i	1012	N/m
E	$2x10^{11}$	N/m^2	L_i	0.2	m
ε	$1x10^{-5}$	m	b_{ti}	0.006	m
φ	0	rad	h	0.003	m
			L_{ti}	0.03	m
			r_{ti}	0.015	m
			I_{ti}	$7.575x10^{-6}$	kg m^2
			E	$2x10^{11}$	N/m^2
			I_i	$1.35x10^{-11}$	m^4

** Due to the tip mass attached to the blade.*

The goal of this study is to understand the effects that a crack brings to the rotor-blade system. In this context, an instability analysis is interesting. Ogata (2002) proposed the method used for this analysis. This method requires the eigenvalues of the system. If the corresponding imaginary part of the eigenvalue is higher than zero, the system is unstable. In the present work, this study was performed by varying the rotation speed of the system from 0 to 5000 RPM and the crack depth from 0 to 50% of the blade height. From Fig. 3, it can be observed that the system is unstable for certain operating conditions and crack severities, mainly for higher crack depths.

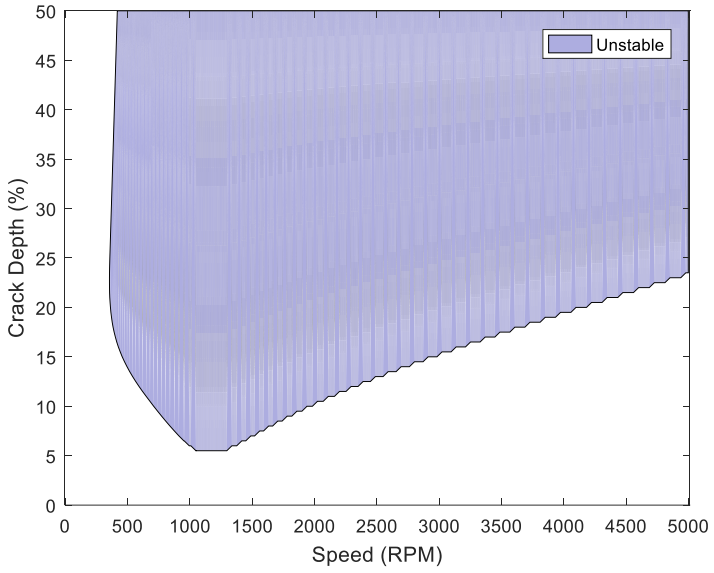

Figure 3: Stable and unstable regions of the system.

Figure 4 shows the system vibration responses obtained by considering the system operating at 300 and 900 RPM for the health, 25% crack depth, and 50% crack depth conditions. At 300 RPM, the system is stable any crack depth. At

900 RPM, the system is unstable for the considered crack depths. Table 2 presents the parameters associated with the crack model.

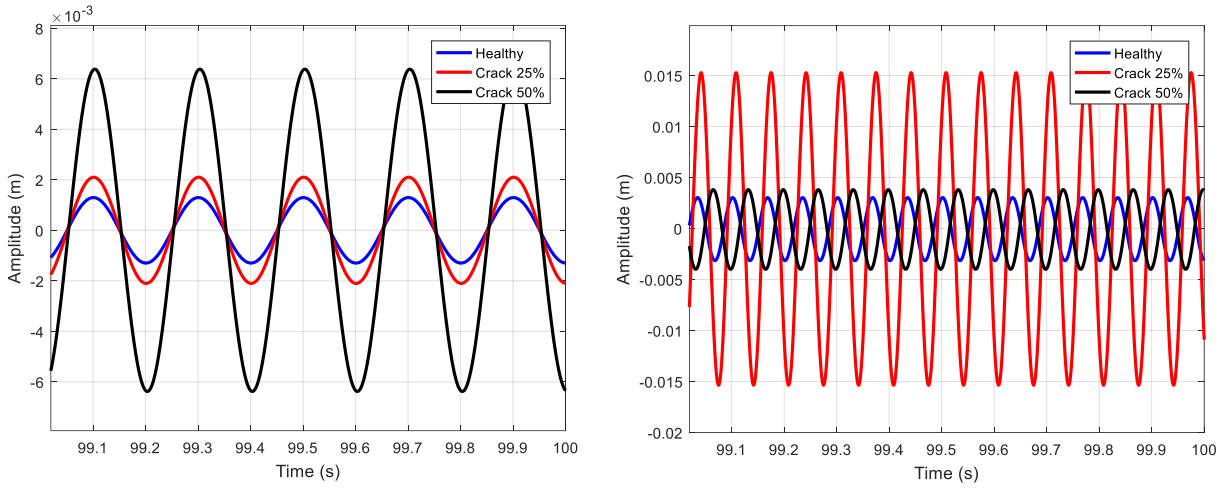

(a) 300 RPM (b) 900 RPM

Figure 4: Time domain responses for the blade #1.

Table 2. Parameters regarding the crack model.

Pristine			*Crack with 25% of depth*			*Crack with 50% of depth*		
k_{eq}	1012	N/m	k_{eq}	650	N/m	k_{eq}	261	N/m
a	0		a	0.25		a	0.5	
$L_{B1} = L_1$	0.2	m	$L_{B1} = 0.05\ L_1$	0.01	m	$L_{B1} = 0.05\ L_1$	0.01	m
L_{B2}	0	m	L_{B2}	0.19	m	L_{B2}	0.19	m

Additionally, the effect of a crack in the blade #1 was evaluated in the natural frequency of the rotor blade system through frequency responses functions (FRFs) obtained for the blade #1. Figure 5 presents the waterfall diagrams, in which the FRFs are obtained according to the rotation speed of the rotor blade system. The curves *A* and *C* represent the natural frequencies for the blade with 25% and 50% crack depths, respectively. The curves *B* and *D* correspond to the same natural frequency of the healthy system. Note that the difference between the curves increases according to the crack depth. As expected, the natural frequency of the system with a crack is smaller than the one of corresponding to the healthy system. Figure 6 clarifies the differences observed between the natural frequencies.

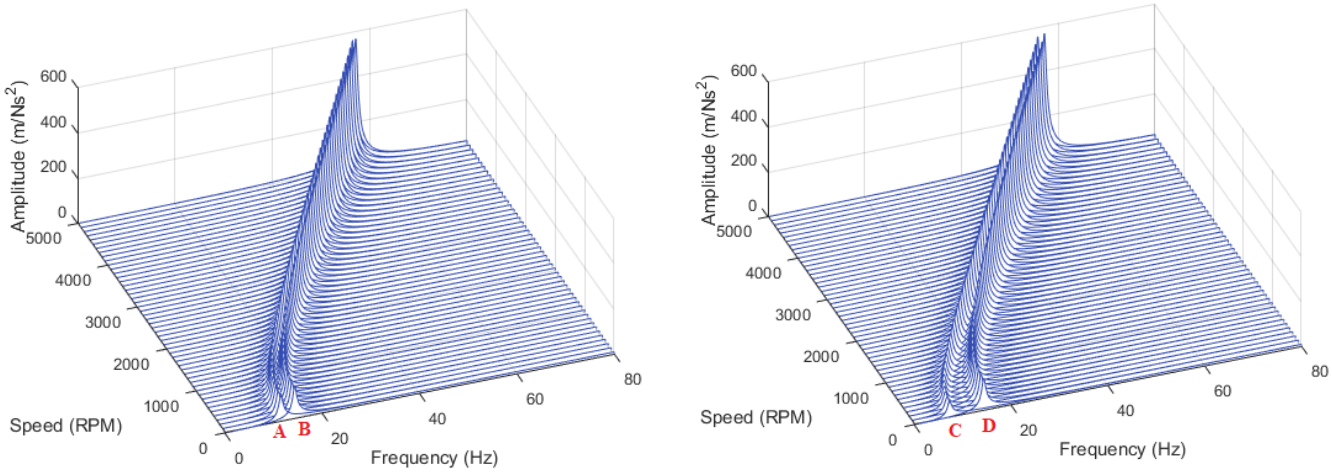

(a) 25% crack depth. (b) 50% Crack depth.

Figure 5: Waterfall diagram for the blade #1 for two different crack depths.

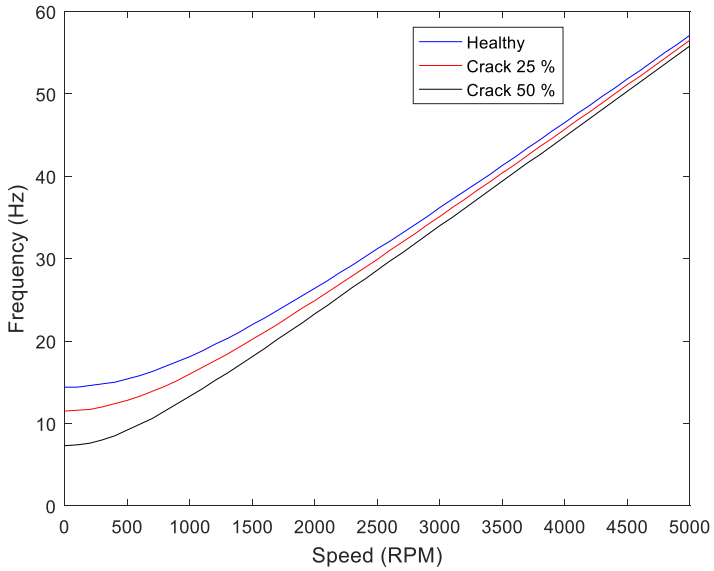

Figure 6: The variation of the natural frequency of the blade #1 for the three crack scenarios.

5. FINAL REMARKS

It is well known that rotating machines coupled with blades may operate under dangerous conditions, which can lead to the growth of cracks. The presence of cracks is undesirable because it may lead to the failure of the system. Thus, it is necessary to apply predictive maintenance techniques as based on vibration responses to ensure safety operating conditions of these machines. In this context, this contribution demonstrated the effects that a crack introduced in a blade of the rotor system has on its dynamic behavior. From the results, it was observed that the crack introduced local flexibility that makes the system unstable. The natural frequencies and the time vibration responses of the system were also evaluated. Further research effort will be dedicated to the experimental verification of the presented results.

6. ACKNOWLEDGEMENTS

The authors are thankful to the Brazilian Research Agencies CAPES, CNPq (574001/2008-5) and FAPEMIG (TEC-APQ-022284-15 / TEC-APQ-307609) for the financial support provided to this research effort.

7. REFERENCES

Chondros, T.G, 1977. *Dynamic response of a cracked beam*, University of Patras, Greece. M. Sc. Thesis.

Dimarogonas A.D, 1976. *Vibration Engineering*. St. Paul, Minnesota, West Publishers.

Dimarogonas A.D. and Paipetis S.A., 1983. *Analytical methods in rotor dynamics*. London, Elsevier Applied Science.

Dimarogonas A.D., Rizos P.F., Aspragathos N., 1990." Identification of crack location and magnitude in a cantilever beam from the vibration modes. In *Journal of Sound and Vibration*, Vol. 138, p. 331-338.

Kane T.R., Ryan R.R., Banerjee A.K., 1987. "Dynamics of a cantilever beam attached to a moving base". In *Journal of Guidance Control and Dynamics*, Vol. 10 (2), p. 139-151.

Legrand, M., 2005. *Modèles de prèdiction de l'interaction rotor/stator dans un moteur d'avion*. Doctorat, thesis, L'École Centrale de Nantes et l'Université de Nantes, Nantes.

Mayes, I.W. and Davies, W.G.R., 1984. "Analysis of the response of a multi-rotor-bearing system containing a transversal crack in a rotor". In *Journal of Vibration, Acoustic, Stress, and Reliability in Design*, Vol. 106, p. 139-146.

Ogata, K., 2002. *Modern Control Engineering*, Prentice Hall, 4th Edition.

Santos, I.F., Saracho, C.M., Smith, J.T., Eiland, J., 2004. "Contribution to experimental validation of linear and non-linear dynamics models for representing rotor-blade parametric coupled vibrations". In *Journal of Sound and Vibration*, Vol. 271, p. 883-904.

Saracho, C.M., 2002. *Numerical and Experimental Analysis of flexible blade dynamic behavior*. Campinas State University. Thesis (Doctorate), Campinas.

Saavedra, P.N., Cuitiño, L. A, 2001. "Crack detection and vibration behavior of cracked beams". In *Journal Computers and Structures*, Vol. 79 (2001), p. 1451-1459.

Simo JC, Vu-Quoc L, 1986. “On the dynamics of flexible beams under large overall motion - the plane case”. Part I and II. In *ASME Journal of Applied Mechanics*, Vol. 53, p. 849-863.

Wu, M.C., Huang, S.C., 1998. “On the vibration of cracked rotating blade”. In *Journal Shock and Vibration*, Vol. 5, p. 317-323.

Xu, H., Chen, Z., Xiong, Y., Yang, Y., Tao, L., 2016. “Nonlinear dynamic behaviors of rotated blades with small breathing cracks based on vibration power flow analysis”. In *Journal Shock and Vibration*, Vol. 2016.

8. RESPONSIBILITY NOTICE

The authors are the only responsible for the printed material included in this paper.